Journal of Sustainable Development Indicators

http://www.sdewes.org/jsdi

Year 2026, Volume 2, Issue 1, 2030681

Original Research Article

Optimal Operation Scheduling of a Battery Swapping Station (BSS) Integrated with Photovoltaic

Tomas Valldeperas Moliné[1], Marko Keber[1], Massimiliano Renzi[1], Jacopo C. Alberizzi[*1]

[1]Faculty of Engineering, Free University of Bozen - Bolzano, via - Bruno Buozzi - Straße 1, 39100 Bozen – Bolzano, Italy

e-mail: tomas.valldeperasmoline@student.unibz.it, marko.keber@unibz.it, massimiliano.renzi@unibz.it, jacopocarlo.alberizzi@unibz.it

Cite as: Valldeperas Moliné, T., Keber, M., Renzi, M., Alberizzi, J. C., Optimal Operation Scheduling of a Battery Swapping Station (BSS) Integrated with Photovoltaic, J. sustain. dev. indic., 2(1), 2030681, 2026, DOI: https://doi.org/10.13044/j.sdi.d3.0681

ABSTRACT

Battery Swapping Stations can significantly reduce electric vehicle refuelling time, but their integration with renewable energy sources requires advanced operational strategies to manage price variability and grid constraints. This study investigates the optimal operation of a Battery Swapping Station integrated with a photovoltaic power plant, aiming to improve economic performance and energy management efficiency. A mixed-integer linear programming optimization model is developed to simulate year-long operations with 15-minute resolution, accounting for battery state-of-charge constraints, swap demand, electricity prices, and photovoltaic generation. A real-world case study of a Charging Point Operator in northern Italy is used for validation. Results show that optimized scheduling shifts battery charging to low-price periods, increases photovoltaic self-consumption, and reduces total energy costs by approximately 56% compared to a non-optimized baseline. The proposed framework provides a novel, practical tool for integrating BSSs with renewable energy, supporting cost-effective and sustainable deployment.

KEYWORDS

Electric vehicles (EVs), Battery swapping, Energy services, MILP optimization, Renewable energy.

INTRODUCTION

The release of greenhouse gases (GHGs) into the atmosphere is a significant driver of global warming [1]. The transportation sector, heavily reliant on fossil fuels, is a major contributor to global emissions, with an average annual growth rate of 1.7% [2]. Road transportation, consuming approximately 2000 Mtoe annually, accounts for nearly 50% of total oil consumption across all sectors. Over the past five decades, road transportation's oil demand has nearly tripled, raising sustainability concerns [3].

Electrification, particularly through the adoption of battery electric vehicles (BEVs), is crucial for decarbonizing transportation. BEVs produce zero tailpipe emissions, and their lifecycle emissions will continue to decrease as renewable energy sources (RES) play a larger role in power generation [4]. Achieving the goal of limiting the global temperature rise to 1.5 °C requires EVs to account for 60% of total vehicle sales by 2030 [5]. The integration of EVs into the transportation sector offers numerous benefits beyond reducing GHG emissions.

* Corresponding author

Electric power as a transportation fuel eliminates tailpipe emissions, can be sourced from renewable and non-emitting energy generation, and offers lower operating costs [6].

EVs utilize existing electric grid infrastructure for recharging, facilitating adoption. Vehicle-to-Grid (V2G) technology allows EVs to serve as mobile energy storage units, enabling energy to flow back to the grid during peak demand periods. This technology contributes to load balancing, voltage regulation, and frequency stabilization [7]. Aligning EV charging with periods of high renewable energy availability reduces curtailment and enhances grid sustainability [8]. Socioeconomic benefits include enhanced national energy security by reducing reliance on imported fossil fuels, noise reduction, improved air quality in cities, and lower overall transportation costs [9].

Despite these advantages, challenges hinder EV adoption. Increased charging demand can strain the electricity grid, necessitating infrastructure upgrades [10], [11]. The high upfront cost of EVs remains a barrier, while extended wait times at charging stations and limited charging options discourage adoption. Battery swapping emerges as an innovative solution, allowing EVs to quickly replace depleted batteries with fully charged ones, reducing wait times and alleviating range anxiety [12]. The battery swapping concept was first introduced in 2007 by the Israeli company Better Place and later fully developed in China by NIO.

While China already has a large network of Battery Swapping Stations (BSSs), the infrastructure in Europe remains underdeveloped. As of now, NIO operates over 2,300 battery-swapping stations worldwide, including 30 in Europe, all located in Northern Europe [13]. However, the company plans to expand its network to six additional European countries: Austria, Belgium, France, Italy, Switzerland, and the UK, positioning BSS technology as a potential alternative to conventional charging stations in the future [14]. BSSs provide fully charged batteries in under five minutes and mitigate renewable energy curtailments by integrating variable renewable energy into grids [15].

A key advantage of battery swapping is the use of batteries housed at swapping stations for offering energy services [16]. While research on energy storage systems often focuses on frequency regulation and grid applications [17], BSS energy services can be classified into three categories: ISO/RTO services for Independent System Operators [18]; utility services for grid operators, including voltage regulation and battery storage integration [19]; and customer services for enterprises, such as demand charge reduction and increased photovoltaic (PV) self-consumption.

To effectively deliver these services, BSS operations must be optimally managed and integrated into smart grids. This requires accounting for variables like EV arrivals, energy needs, supply and demand dynamics, power system behaviour and renewable energies integration.

For instance, in [20], the authors introduce a unified mixed-integer programming framework for EV service network design that integrates battery swapping and recharging under capacity constraints.

The study [21] analyses PV hosting capacity in distribution grids with EV battery swap stations under centralized and decentralized modes.

In this context, advanced optimization methods are critical for achieving optimal outcomes [22]. The objective of this paper is to apply a mixed-integer linear programming (MILP)-based optimization model for the year-round operational scheduling of a BSS integrated with a photovoltaic power plant. The proposed framework aims to minimize total operating costs while maximizing economic benefits by optimally managing battery charging, grid energy exchanges, and PV self-consumption under realistic Italian electricity tariff structures. By jointly modelling BSS operation, a conventional charging station, and photovoltaic generation, the study seeks to provide a practical decision-support tool for Charging Point Operators operating under real-world technical, economic, and regulatory constraints.

The study contributes to the United Nations Sustainable Development Goals, particularly SDG 11 (Sustainable Cities and Communities) and SDG 13 (Climate Action) by supporting the

deployment of fast and reliable electric vehicle refueling infrastructure in urban environments. Optimized load management and peak power reduction enhance grid resilience and facilitate the integration of electric mobility within existing urban energy systems, contributing to more sustainable and resilient cities.

In addition, the framework promotes climate action by increasing photovoltaic self-consumption, reducing energy withdrawals from the grid, and shifting battery charging toward periods with lower electricity prices and typically higher renewable energy availability. These effects contribute to lower indirect greenhouse gas emissions associated with electric vehicle operation and support the decarbonization of the transport sector.

Novelty and Contributions

Despite the growing literature on BSS and renewable energy integration, several important gaps remain. Most existing studies focus either on conventional EV charging stations or on BSSs modelled as standalone systems, without jointly considering their integration within a shared grid connection. Moreover, many contributions rely on simplified electricity price assumptions, neglecting real tariff structures that include power demand charges, grid fees, and time-varying market prices.

Compared to V2G and stationary storage integration studies, the proposed framework explicitly accounts for the operational logic and service constraints of battery swapping, which differ substantially from flexible EV charging or generic storage dispatch.

From a methodological perspective, recent studies have started to explore artificial intelligence and machine learning techniques for energy management and scheduling problems [23]. While these approaches are effective for forecasting and pattern recognition, they typically require large training datasets, offer limited interpretability, and do not guarantee globally optimal solutions under strict operational constraints. In contrast, MILP techniques provide a deterministic and transparent optimization framework, ensuring global optimality while explicitly accounting for technical, economic, and regulatory constraints. This makes MILP particularly suitable for this kind of problems where non-linearities are not particularly relevant like in the infrastructure planning and operational optimization problems involving BSSs and grid-connected renewable energy systems.

In this context, the main contribution of this paper is the development of the comprehensive MILP-based optimization framework. By integrating high-resolution demand data, realistic electricity prices, and detailed battery operational constraints, the proposed approach provides practical insights into cost reduction, load shifting, and renewable energy utilization for Charging Point Operators.

Many studies have highlighted the significant advantages of integrating PV systems into battery charging infrastructures, particularly regarding the reduction of greenhouse gas emissions and the enhancement of system resilience [24].

By locally generating electrical energy from renewable sources, PV plants contribute to strengthening the overall energy system, making it less susceptible to market price fluctuations [25].

However, the inclusion of additional variables also increases system complexity, thereby requiring the development of advanced tools and methods for effective management.

MATERIALS AND METHODS

Problem Definition

To optimally manage the energy flows within this system, a dedicated tool has been developed, incorporating two optimization solvers as shown is **Figure 1**. Specifically, the tool employs a MILP approach to determine the optimal scheduling of battery charging and the distribution of PV energy between self-consumption and grid injection, with the overarching goal of maximizing total system revenues.

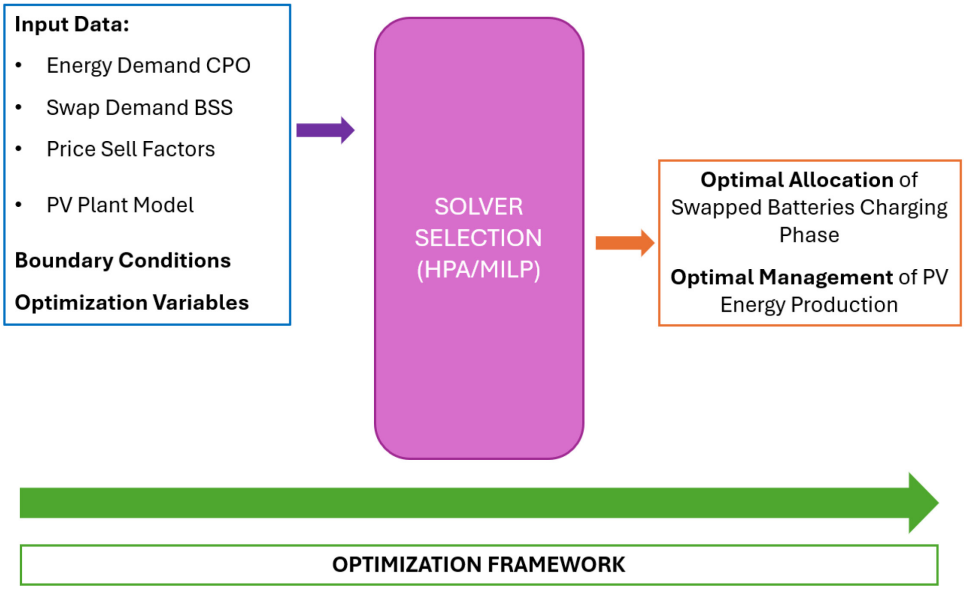

Figure 1. Optimization framework

Optimization Method

An optimization problem typically consists of three fundamental components: an objective function, a set of decision variables, and a set of constraints that define the feasible solution space. The optimization algorithm aims to determine the optimal value of the objective function by assigning suitable values to the decision variables while satisfying all the imposed constraints [26].

In the context of heuristic and metaheuristic techniques, their application to energy system scheduling problems has been extensively documented in the literature. However, their main limitation lies in the fact that they do not guarantee global optimality and may converge to suboptimal solutions [27].

On the other hand, MILP techniques are iterative optimization methods that, compared to heuristic-based algorithms, typically require higher computational resources. Nonetheless, MILP approaches are supported by robust solvers and solid mathematical foundations, which ensure solution reliability and guarantee optimality within a well-defined tolerance.

In this study a MILP model has been implemented in Python through the PuLP library within the Spider programming environment [28]. The model is solved using the GLPK solver. It was selected due to its robustness, transparency, and suitability for large-scale linear optimization problems. The formulation is solver-independent and can be readily implemented using commercial solvers such as Gurobi or CPLEX if available. All simulations were performed on a standard workstation equipped with an Intel® Core™ i7 processor (3.2 GHz) and 16 GB of RAM. The year-long MILP optimization with 15-minute resolution was solved within a few minutes of computational time, demonstrating the practical feasibility of the proposed approach for operational and planning applications.

Objective function. The objective function of the proposed optimization problem is to minimize the total annual operating cost of the integrated system, including energy purchase costs, grid power demand charges, and revenues from photovoltaic energy injection into the grid.

$$\mathrm{OF} = \min\left\{P_{\mathrm{p}} \times F_{\mathrm{p}} + \sum_{i:1}^{N}\left[E_{\mathrm{g}}(i) \times \left(F_{\mathrm{e}}(i) + F_{\mathrm{ge}}(i)\right) - PV_{\mathrm{inj}}(i) \times F_{\mathrm{inj}}(i)\right]\right\} \quad (1)$$

where i is the timestep, P_{p} [kW] the peak power demand during the billing period, F_{p} [EUR/kW] the peak power fee, $E_{\mathrm{g}}(i)$ [kWh] the energy withdrawn from the grid at timestep i,

$F_e(i)$ [EUR/kWh] the price of energy withdrawn from the grid, $F_{ge}(i)$ [EUR/kWh] the grid fee for withdrawn energy, $PV_{inj}(i)$ [kWh] the energy injected into the grid at timestep i and $F_{inj}(i)$ [EUR/kWh] the price of energy injected into the grid. The objective function consists thus of two main components. The first is the power cost, which refers to the cost associated with the maximum contracted power that can be supplied by the electrical grid. The second component is the energy cost, which is the cost related to the energy drawn from or injected into the grid during each time step. This cost is calculated by multiplying the energy by its price.

Problem constraints – MILP formulation. In optimization problems, constraints establish boundary conditions for the variables influencing the objective function. In Mixed-Integer Linear Programming (MILP) problems, these constraints must be linear equalities or inequalities. For this optimization problem, constraints include energy balance and battery operations. The energy balance constraint ensures that grid and photovoltaic supply, and battery charging/discharging match energy demand at each time step. Battery constraints limit charge/discharge power and enforce state of charge (SOC) limits to protect battery lifetime.

$$\sum_{i=1}^{N}\left(E_{\mathrm{g}}(i)+PV_{\mathrm{l}}(i)\right)=\sum_{i=1}^{N}\left(E_{\mathrm{d}}(i)+\left(B_{\mathrm{ch}}(i)-B_{\mathrm{dh}}(i)\right)\right) \tag{2}$$

Eq. (2) is an energy balance constraint that ensures the total energy supplied and stored matches the demand for each time period. It states that the sum of electricity drawn from the grid ($E_g(i)$) and energy produced by the PV power plant ($PV_l(i)$) must equal the total energy demand ($E_d(i)$) plus the net energy used for battery charging ($B_{ch}(i)$ - $B_{dh}(i)$), accounting for charge-discharge efficiency losses.

$$0 \leq P_{\mathrm{B_{ch}}}(i) \leq P_{\mathrm{grid}}(i) \tag{3}$$

$$0 \leq P_{\mathrm{B_{dh}}}(i) \leq P_{\mathrm{B_{MAX}}} \tag{4}$$

$$0 \leq B_{\mathrm{SOC}}(i) \leq B_{\mathrm{C}} \tag{5}$$

$$B_{\mathrm{SOC}}(i)=B_{\mathrm{SOC}}(i-1)+B_{\mathrm{ch}}(i)-B_{\mathrm{dh}}(i) \tag{6}$$

$$B_{\mathrm{dh}}(i)=B_{\mathrm{SWAP}}(i) \tag{7}$$

$$PV(i)=PV_{\mathrm{l}}(i)+PV_{\mathrm{inj}}(i) \tag{8}$$

Eq. (3) limits the battery charging power (P_{Bch}) to not exceed the power delivered by the grid (P_{grid}). Eq. (4) limits the battery discharging power (P_{Bdh}). Eq. (5) ensures the state of charge of the battery (B_{SOC}) remains within the allowable range, preventing overcharging and over-discharging. Eq. (6) describes how SOC changes with charging and discharging at each time step. Battery charging and discharging processes are modelled using constant efficiencies assumed to be equal for all batteries and constant over time. A round-trip efficiency is assumed and split equally between charging and discharging phases. Battery degradation effects are not explicitly modelled, as the focus of this study is on short- to medium-term operational optimization rather than lifetime degradation.

Eq. (7) states that a swap order results in a fully charged battery being exchanged with a drained one, decreasing the overall SOC of the battery stack. Eq. (8) is the energy balance

constraint over the total PV production that must equal the sum of the PV energy delivered to the load (PV_{l}) and to the grid (PV_{inj}).

Optimization variables – MILP formulation. The optimization variables determine the final value of the objective function, and their value is computed by the algorithm to minimize the latter. In this case, the optimization variables are P_{p}, E_{g}, B_{ch}, PV_{inj} and PV_{l}.

Models' variables and parameters used in the optimization problem are listed in **Table 1**.

Table 1. Model variables and parameters

Symbol	Description	Unit	Bounds
$E_{\mathrm{g}}(i)$	Energy withdrawn from the grid at time step i	kWh	≥ 0
$PV_{\mathrm{inj}}(i)$	Energy injected into the grid at time step i	kWh	≥ 0
$PV_{\mathrm{l}}(i)$	PV energy directly supplied to the load	kWh	≥ 0
$B_{\mathrm{ch}}(i)$	Battery charging energy at time step i	kWh	≥ 0
$B_{\mathrm{dh}}(i)$	Battery discharging energy at time step i	kWh	≥ 0
$B_{\mathrm{SOC}}(i)$	State of charge of the battery stack	%	[$\mathrm{SOC}_{\mathrm{min}}$, $\mathrm{SOC}_{\mathrm{max}}$]
P_{p}	Peak power demand during billing period	kW	≥ 0
F_{p}	Power demand fee	EUR/kW	Given
$F_{\mathrm{e}}(i)$	Electricity price at time step i	EUR/kWh	Given
$F_{\mathrm{ge}}(i)$	Grid fee for withdrawn energy	EUR/kWh	Given
$F_{\mathrm{inj}}(i)$	Selling price for injected PV energy	EUR/kWh	Given
$P_{\mathrm{B}_{\mathrm{ch}}}(i) - P_{\mathrm{B}_{\mathrm{dh}}}(i)$	Max battery charge - discharge power	kW	Given

Case Study

The model was tested in a case study involving a CPO planning the installation of a new charging station alongside a 500 kWp photovoltaic (PV) power plant near an existing BSS. The new charging station includes four high-power chargers; each rated at 100 kW. The nearby BSS is designed with 21 battery slots, enabling swaps in under five minutes and supporting the charging of more than ten batteries per hour. To meet peak power requirements, the BSS is connected to the grid with a 600-kW capacity, operating around 50 battery swaps per day. The overall system configuration is shown in **Figure 2**.

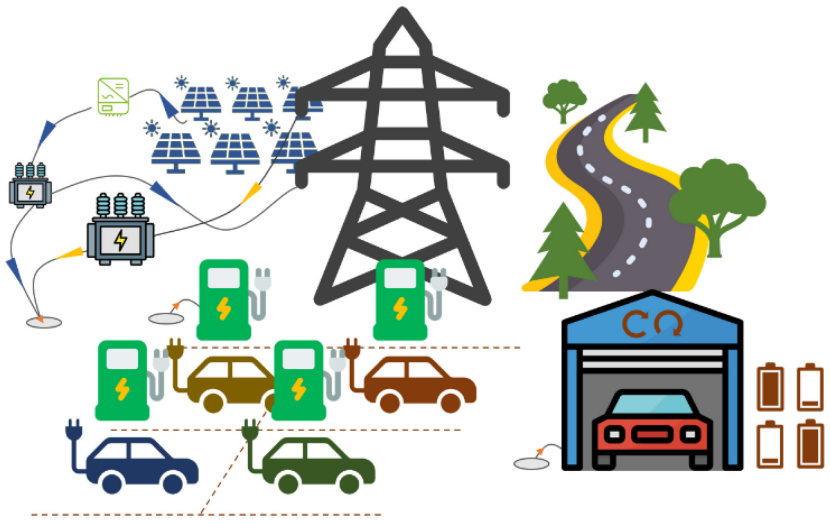

Figure 2. Energy system configuration

Charging Point Operator (CPO) Model. **Figure 3** illustrates the typical daily energy demand profile of the charging station, where multiple vehicles may concurrently use one or more charging points. While the original dataset contains quarter-hourly data for the entire year, the graph presents the average and maximum power demand for each 15-minute interval of a representative day, providing a clearer view of demand dynamics. The average demand curve indicates low power consumption during nighttime hours (1:00 AM – 6:00 AM), followed by a gradual rise in the early morning. Demand increases significantly after 9:00 AM and reaches its highest levels between 12:00 PM and 3:00 PM, when up to four vehicles may charge simultaneously. The maximum demand curve captures fluctuations caused by both the number of active charging sessions and the maximum power drawn per vehicle. Although the theoretical upper limit is 400 kW, this level is seldom reached, suggesting that full-capacity charging events are relatively rare.

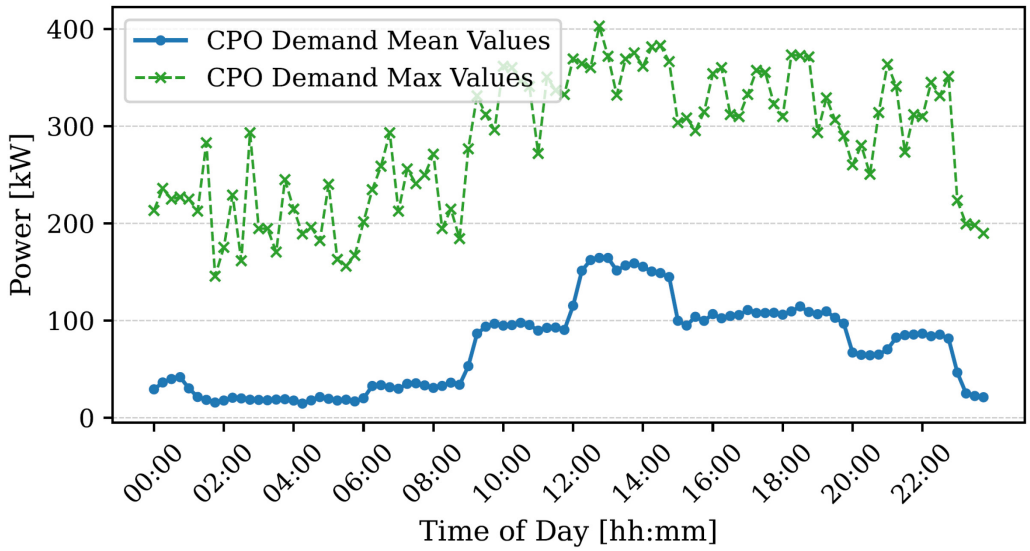

Figure 3. Mean and maximum values for charging station power demand

Battery Swapping Station (BSS) Model. The literature was reviewed to support the key assumptions regarding the operational behavior of the Battery Swapping Station (BSS), to develop an appropriate operational model, and to evaluate battery availability under typical daily conditions. The review first aimed to identify the periods of peak activity when battery swaps are most likely to occur [29]. The main assumptions concern the distribution of daily swaps [30] and the energy required for recharging the batteries.

A representative daily swap pattern reveals low activity during the early morning hours, increasing before noon, peaking in the afternoon, and then gradually declining until a secondary peak occurs around 9 – 10 PM. **Figure 4** illustrates this pattern, showing that swaps generally start around 7 AM, with minimal or no activity overnight due to station closures or reduced demand. The figure also presents the average hourly electricity price for the years 2020–2024, computed using eq. (9) by averaging the hourly recorded prices across the entire period.

$$\text{for } i = 1{:}24, E_i = \frac{\sum_{j:1}^{365} E_{i,j}}{365} \tag{9}$$

In terms of power demand, and in the absence of a smart charging strategy, energy consumption is assumed to follow the swapping pattern, as batteries are recharged immediately after each swap to ensure continuous availability. The total daily energy requirement for 50 swaps is estimated to range between 2500 and 2800 kWh, corresponding to an average of

approximately 55 kWh per swap. This estimate is based on a typical 100 kWh battery, such as that used in a fully electric SUV [31], with the State of Charge (SOC) maintained between 20% and 80% to optimize battery lifespan.

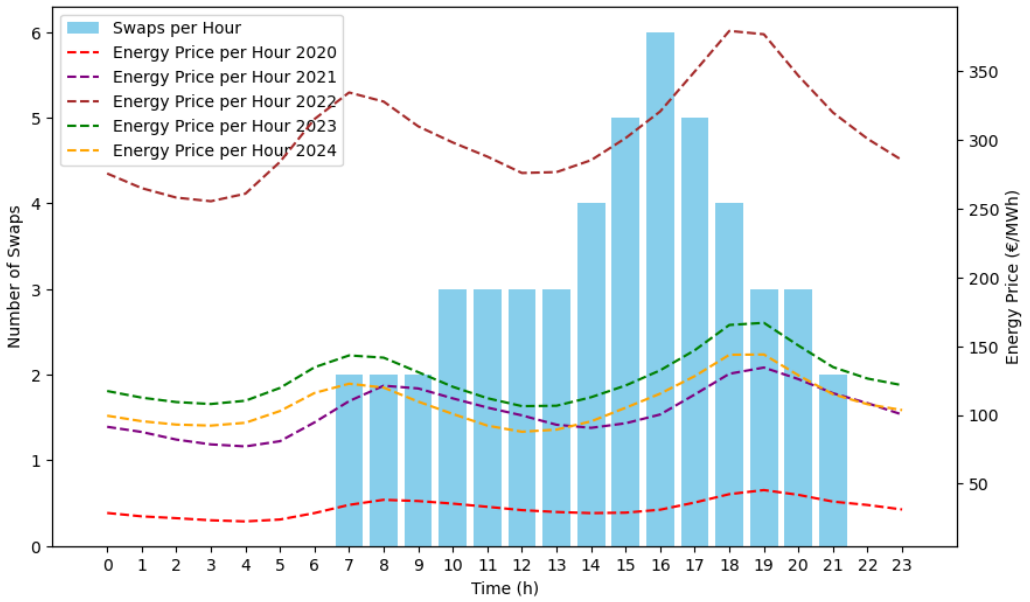

Figure 4. Battery swaps per hour and average energy price throughout the day

The operation of the BSS was simulated using a linear programming algorithm designed to allocate swap requests to available batteries while optimizing overall power demand. The main objective was to determine the minimum number of batteries required to satisfy daily swap requests or to complete all swaps within a predefined power capacity limit. The algorithm thus optimizes BSS operation by minimizing peak power drawn from the grid while ensuring that all daily battery swaps are fulfilled. It evaluates the trade-off between the number of batteries and the peak grid demand: a smaller battery stock leads to higher peak demand due to concurrent charging requirements, whereas a larger number of batteries reduces peak demand but increases infrastructure and investment costs.

The model was developed based on the following assumptions:

- No swaps between 12:00 AM and 08:00 AM.
- Batteries in the BSS have a total capacity of 100 kWh, typical of a full electric SUV.
- Batteries are numbered from 1 to the total number (13 or 21) and swapped sequentially, when the last available battery is reached, the counter is restarted.
- Energy provided with each swap is on average 55 kWh ranging between 50 kWh and 60 kWh.
- Maximum battery charging power is 60 kW, so a battery can be charged and be available to swap in around 1 hour.
- A maximum of 2 swaps can be performed in a 15-minute period (8 per hour).

The model was subsequently executed multiple times with swap requests randomly distributed over the day. This stochastic approach was adopted to validate the robustness of the BSS operation, ensuring that performance remained consistent regardless of the specific characteristics of the swap demand curve.

The simulation results are presented in **Figure 5**. Initially, the analysis considered two existing BSS configurations, one with 13 batteries and another with 21 batteries. The results

were then compared to assess the benefits of additional batteries in mitigating overall power demand.

It was observed that for low daily swap volumes (below 40 swaps per day), the required power demand was nearly identical in both configurations. This indicates that increasing the number of batteries does not provide any tangible advantage, as power management is already optimized under these conditions. During nighttime hours, when there is no swapping activity, the limited charging power prevents additional batteries from being fully charged. For example, with a maximum station power of 60 kW, only one battery can be charged at a time, allowing for a total of 8 batteries to be charged between 12:00 AM and 08:00 AM.

Consequently, a maximum of 24 batteries can be charged within a full day, enabling up to 24 swaps, assuming the availability of at least 8 batteries. If exactly 24 swaps are performed, any batteries beyond the initial 8 remain unused or serve as operational reserves. This scenario is only valid if swap events are evenly distributed during the day; otherwise, higher charging power would be required to maintain service continuity.

When the daily swap count exceeds 40, the system with 13 batteries requires an additional 45 kW of power to sustain operations. Beyond 50 swaps per day, operational constraints emerge due to the maximum allowable swaps per hour, necessitating either a significant power increase or additional batteries. Once daily swaps exceed 50, the advantage of having more batteries becomes evident, as a larger storage capacity allows for night-time charging and smoother power distribution. For instance, with an installed power of 300 kW, a 13-battery configuration can support approximately 80 swaps per day, whereas a 21-battery configuration can accommodate over 100 swaps.

On the other hand, experiments with an 8-battery setup showed that up to 30 daily swaps can be achieved with nearly the same power demand, while 40 daily swaps require around 150 kW of available capacity. Moreover, with sufficient grid power, a high number of swaps can still be performed even with a relatively small number of batteries. For example, a 13-battery configuration connected to a 450 kW supply can support more than 130 swaps per day. This finding suggests that the redundancy in the number of available batteries is relatively low, typically less than 10% of the total circulating batteries, and even lower when considering that the average user performs only a few swaps per month.

In this study, the selected BSS model features 21 battery slots and enables battery swaps in under 5 minutes, supporting the charging of more than 10 batteries per hour. Accordingly, such installations are designed with a 600 kW grid connection capacity. The maximum and average daily power demand profiles for the BSS are illustrated in **Figure 6**.

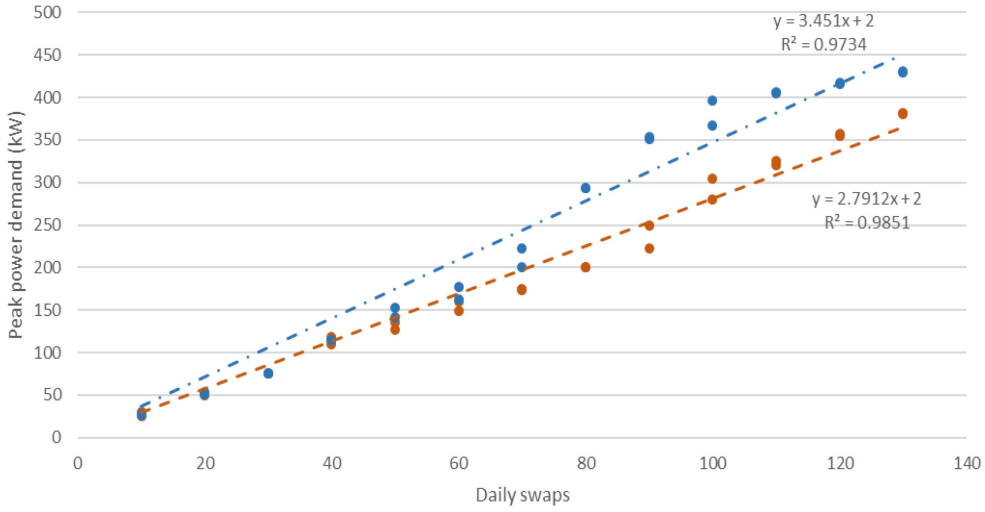

Figure 5. Daily swaps and maximum power demand for 2 configurations

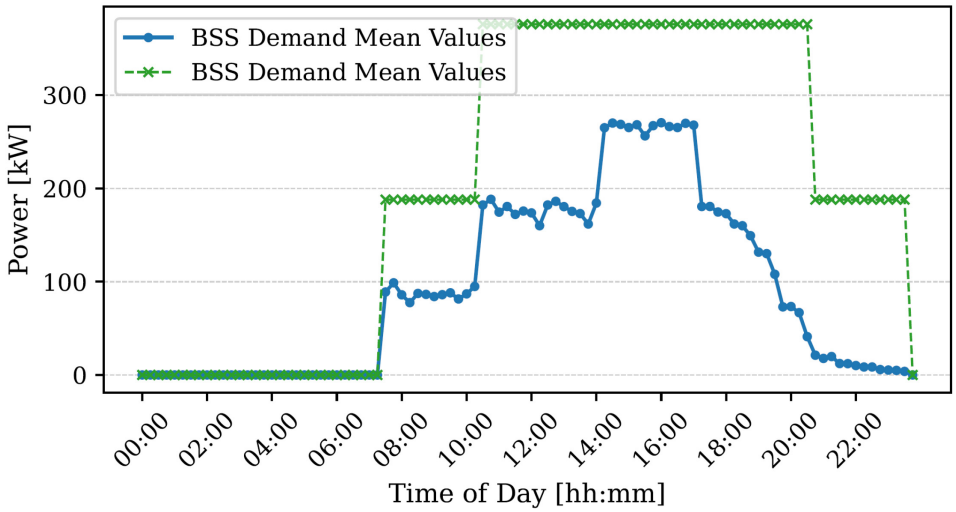

Figure 6. Maximum and average daily power demand for the BSS and the charging station

Photovoltaic (PV) Model. The photovoltaic (PV) system was modelled according to [32], using a poly-crystalline module with a net cell opening area (A_{eff}) of 1.82 m², an efficiency of 14.6% in Standard Test Conditions (STC) and a peak power of 410 W [33]. The DC power delivered by the PV system was computed using eq. (10), where G is the solar radiation and η_{c} is the cell efficiency, assumed to be equal to the STC efficiency for a simplified model. To calculate the effective AC power produced by the PV system, Balance of System (BOS) losses, which typically reduce DC power by 15%, must be considered. These losses are accounted for in the computation of AC power using eq. (11), with a BOS efficiency (η_{BOS}) assumed to be 85%.

$$P_{\text{PV}}(\text{DC}) = \eta_{\text{c}} \times A_{\text{eff}} \times G \tag{10}$$

$$P_{\text{PV}}(\text{AC}) = P_{\text{PV}}(\text{DC}) \times \eta_{\text{BOS}} \tag{11}$$

Data Sources

The optimization model is based on multiple data sources. Photovoltaic generation profiles are derived from standard PV performance models using site-specific irradiation data. Charging station load profiles are based on measured or representative operational datasets with quarter-hourly resolution. Battery swap demand patterns follow distributions reported in the literature for typical BSS operation. Electricity prices correspond to historical hourly wholesale market data, while grid and management fees are based on regulated Italian tariff structures. All datasets are processed to ensure consistency with the adopted temporal resolution.

RESULTS AND COMMENTS

To validate the model, it was applied to a case study of a CPO based in northern Italy seeking to expand its network by installing a new BSS near its existing charging facilities. **Table 1** outlines the main features of the current charging station scenario, while **Table 2** resents a detailed description of the BSS configuration.

Table 2. Charging station – case study scenario

Daily charging sessions	Charging points	Installed power [kW]	Peak demand [kW]	Annual energy demand [kWh]
60	4	400	403	634,386.00

Table 3. BSS – case study scenario

Battery Slots	Max Swaps per Hour	Installed power [kW]	Peak demand [kW]	Annual energy demand [kWh]
50	10	600	376	826.588

Table 3 outlines the fees that Italian end users must pay for energy, grid access, and management. These include a variable energy fee that depends on the energy withdrawn, a fixed power fee set by the contracted power, and a fixed management fee covering both technical and commercial services.

Table 4. Energy, Grid and Management Fees

Point of Delivery Power [kW]	Energy Fee [EUR/kWh]	Grid Fee [EUR/kW/Month]	Management Fee [EUR/POD/Month]
$P \leq 100$	UNP	2.65	36.41
$100 < P \leq 500$	UNP	2.38	32.77
$P > 500$	UNP	2.09	31.66

The grid and management fees are regulated by the Italian Regulatory Authority for Energy, Networks and Environment (ARERA) [34], whereas the energy fee is linked to the Prezzo Unico Nazionale (PUN), or Unique National Price (UNP), the wholesale electricity reference price on the Italian Power Exchange (IPEX) [35]. UNP is provided as an hourly value; in this study, the average hourly UNP for the years 2020–2024 has been considered, and its trend is illustrated in **Figure 4**.

Assuming that integrating a BSS with the existing charging station under a shared grid connection can enhance load balancing, improve power utilization, and reduce peak capacity requirements, the combined energy demand of the charging station and the BSS has been adopted as the load profile for the optimization process, as shown in **Figure 7**.

In this framework, the power demand profiles of the charging station and the BSS were summed to generate a single aggregated profile, which serves as the input for the optimization algorithm. The resulting aggregated demand exhibits a distinct afternoon peak, while night-time demand remains minimal due to the absence of swaps and the limited number of charging requests.

This pattern creates an opportunity to store energy during off-peak night-time hours, thereby mitigating afternoon and evening demand peaks, periods typically associated with higher grid loads. Consequently, this strategy enables potential cost savings, as energy prices are generally lower during the night.

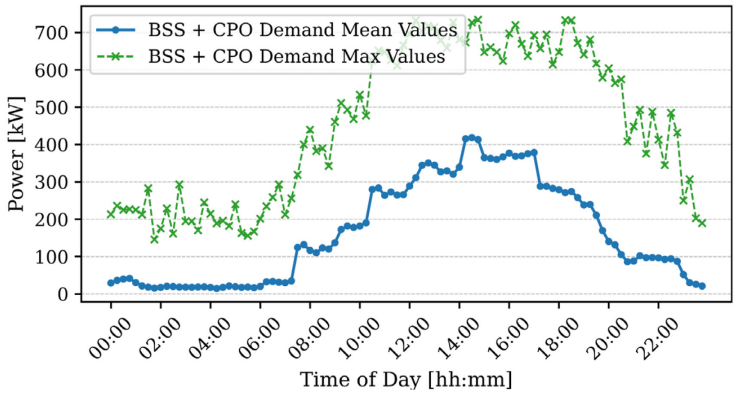

Figure 7. Average daily combined demand of the charging station and a BSS

The optimization process was carried out using year-long demand data, discretized into 15-minute intervals. This time resolution is adopted to balance modelling accuracy and computational tractability.

The optimization was performed using year-long demand, price, and photovoltaic generation data, allowing seasonal effects to be inherently captured. Differences in solar availability and electricity price patterns across seasons influence the absolute magnitude of savings; however, the relative benefits of load shifting, peak power reduction, and increased PV self-consumption remain consistent throughout the year. This confirms the robustness of the proposed approach under varying seasonal conditions.

Total operating expenses depend on the considered UNP, as illustrated in **Figure 4**, together with grid costs, determined by the maximum contracted power, and the management fees reported in **Table 4**.

Figure 8 presents the simulation results based on the UNP for the year 2024. The outcomes indicate a significant shift in energy demand toward night-time hours, corresponding to lower electricity prices, and a marked reduction in the energy withdrawn from the grid. The optimization algorithm adjusts the charging phase of the swapped batteries, increasing energy absorption during periods of low prices.

Figure 9 compares the original and optimized power demand profiles alongside the photovoltaic generation curve, highlighting the PV system's contribution to meeting the total energy requirements. The amount of PV energy directly supplied to the load is influenced by the selling price of electricity. It can therefore be inferred that lower selling prices make self-consumption economically more advantageous.

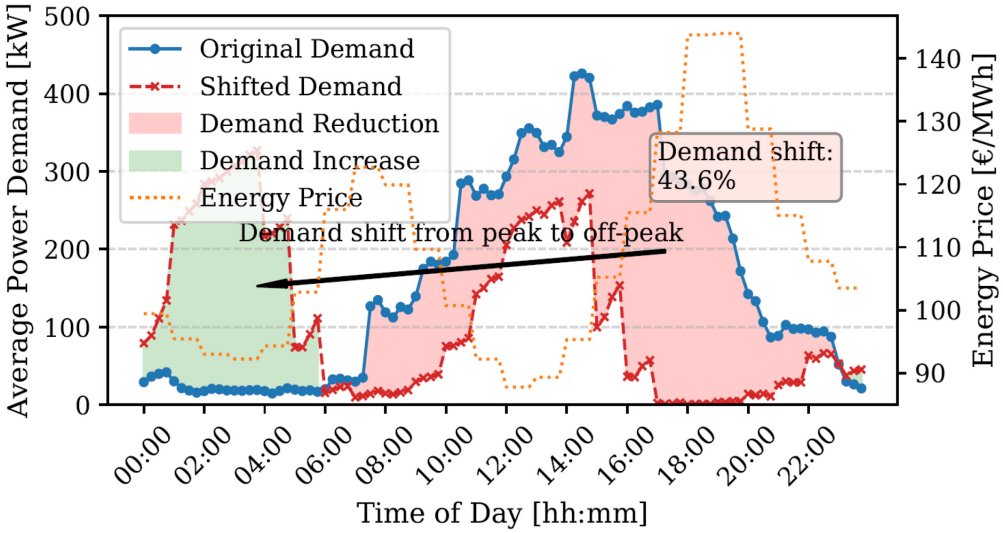

Figure 8. Average and maximum daily combined demand of the CPO and the BSS after the MILP optimization. The baseline scenario refers to non-optimized operation. The optimized scenario corresponds to the MILP-based scheduling strategy

The results demonstrate that the optimization algorithm effectively enhances the utilization of renewable energy by allocating part of the PV output directly to the system load, while exporting surplus energy to the grid. This strategy maximizes total revenue from PV generation.

The total cost obtained through the MILP optimization are reported in **Table 5**. These findings highlight the economic and operational benefits of integrating energy storage and load-shifting strategies and further validate the robustness and effectiveness of the MILP approach in optimizing energy management and minimizing costs.

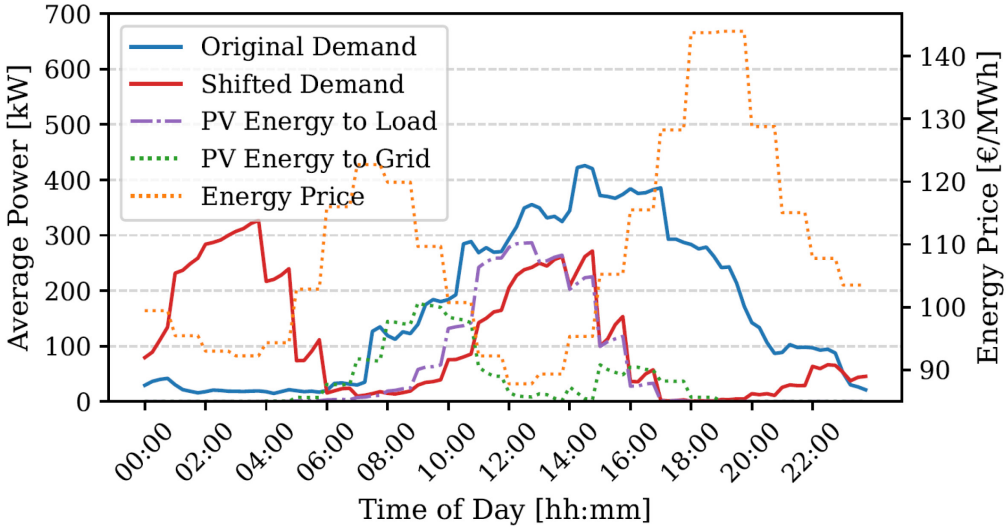

Figure 9. Comparison between baseline and optimized average daily combined power demand of the CPO and BSS, together with photovoltaic energy production

Table 5. Annual cost comparison between baseline and optimized operation

Cost component	Baseline	Optimized	Variation
Energy cost	EUR 162,152.92	EUR 88,718.10	−55%
Peak demand cost	EUR 18,655.00	EUR 10,057.08	−45%
Revenues PV		EUR 33,779.45	

To assess the robustness of the proposed optimization framework and the transferability of the results, a sensitivity analysis was conducted on the installed photovoltaic (PV) capacity. In addition to the base case, a larger PV system of 700 kW_p was evaluated. Increasing the PV capacity enhances the contribution of solar generation to the total energy demand, leading to a reduction in energy withdrawals from the grid and higher revenues from PV energy injection. Conversely, power-related costs, although significantly reduced through the optimization process, exhibit limited variability, as they are less sensitive to changes in PV capacity than energy-related costs. These findings, listed in **Table 6**, confirm that, while the magnitude of economic savings depends on site-specific conditions, the proposed optimization framework remains effective and robust across different system configurations.

Table 6. Sensitivity analysis results

PV Size [kW_p]	PV Energy injected into the grid	PV Energy delivered to the load	Energy Costs reduction	Power Costs reduction
500	37%	63%	55%	45%
700	43%	57%	48%	47%

To facilitate comparison and improve the generality of the results, a normalized performance indicator was introduced alongside absolute economic savings. This indicator allows the assessment of the optimization benefits independently of site-specific scale effects and enable comparison with other studies and deployment scenarios.

The economic benefit was normalized with respect to the total annual energy demand. The optimized configuration achieves an average cost saving of 71 EUR/MWh in case of 500 kW_p

PV plant and 93 EUR/kWh in case of 700 kW_p PV plant, highlighting the effectiveness of the proposed strategy independently of total consumption levels.

Moreover, although the case study focuses on the Italian electricity market, the proposed methodology is fully transferable to other European contexts. Differences in electricity price volatility, power demand charges, and feed-in remuneration schemes are expected to influence the magnitude of economic benefits, but not the overall effectiveness of the optimization strategy. In markets with higher price spreads or stronger incentives for self-consumption, the value of load shifting and PV integration may be even greater, whereas flatter tariff structures may reduce, but not eliminate, the advantages of coordinated BSS operation. The model can be readily adapted by updating tariff inputs and regulatory parameters.

CONCLUSIONS

This study presents a comprehensive optimization framework for the year-round operation of a Battery Swapping Station (BSS) integrated with a photovoltaic (PV) system. By incorporating real-world operational constraints, hourly electricity prices, and PV generation profiles, the proposed methodology demonstrates strong potential to enhance both the economic efficiency and operational performance of integrated BSS–PV systems.

A mixed-integer linear programming (MILP) algorithm is developed to optimize BSS operation while accounting for time-varying energy prices and grid constraints. Simulation results show substantial economic and operational benefits, highlighting the model's ability to exploit electricity price differentials through optimal scheduling. Depending on the installed PV capacity, the optimized strategy reduces energy-related operating costs by approximately 50% compared to a non-optimized baseline while improving overall system efficiency. In addition, the coordinated operation of the BSS and the charging station significantly decreases peak grid power demand, reducing power-related costs by around 45% and improving utilization of the existing grid connection.

A real-world case study of a Charging Point Operator (CPO) in northern Italy demonstrates the practical applicability of the proposed framework. Load-shifting results indicate a marked displacement of energy demand toward night-time periods with lower electricity prices, while enhanced alignment between battery charging and PV generation increases renewable energy utilization. Overall, the results confirm the economic and environmental advantages of integrated BSS–PV systems supported by advanced operational optimization.

ACKNOWLEDGMENTS

This study was carried out within the project "RENoN - Total integration of energy networks and prosumers towards a decarbonized energy infrastructure", supported by the Autonomous Province of Bolzano/Bozen - South Tyrol through the Research Südtirol/Alto Adige 2022 call, under Research Grant No. 1047748, CUP I53C2300249003.

DECLARATION OF GENERATIVE AI AND AI-ASSISTED TECHNOLOGIES IN THE WRITING PROCESS

During the preparation of this work the authors used AI tools to improve language and readability of the paper. After using these tools/services, the authors reviewed and edited the content as needed and take full responsibility for the content of the publication.

REFERENCES

1. European Parliament, Climate change: the greenhouse gases causing global warming, https://www.europarl.europa.eu/topics/en/article/20230316STO77629/climate-change-the-greenhouse-gases-causing-global-warming, [Accessed: Oct. 2, 2025].
2. IEA - International Energy Agency, Transport, https://www.iea.org/energy-system/transport, [Accessed: Oct. 2, 2025].

3. IEA - International Energy Agency, Key world energy statistics 2020, https://www.iea.org/reports/key-world-energy-statistics-2020, [Accessed: Oct. 2, 2025].
4. Umair, M., Hidayat, N. M., Abdullah, E., Hakomori, T., Ahmad, A. S. and Nik Ali, N. H., A Review on Electric Vehicles: Technical, Environmental, and Economic Perspectives, Journal of Sustainable Development of Energy, Water and Environment Systems, Vol. 13, No. 3, pp 1130568, 2025, https://doi.org/10.13044/j.sdewes.d13.0568
5. IEA - International Energy Agency, World Energy Outlook 2023, https://origin.iea.org/reports/world-energy-outlook-2023, [Accessed: Oct. 2, 2025].
6. Borlaug, B., Salisbury, S., Gerdes, M. and Muratori, M., Levelized Cost of Charging Electric Vehicles in the United States. Joule, Vol. 4, No. 7, pp 1479-1485, 2020, https://doi.org/10.1016/j.joule.2020.05.013
7. Zheng, Y., Shao, Z., Shang, Y. and Jian, L., Modeling the temporal and economic feasibility of electric vehicles providing vehicle-to-grid services in the electricity market under different charging scenarios. Journal of Energy Storage, Vol. 68, pp 107579, 2023, https://doi.org/10.1016/j.est.2023.107579
8. Izquierdo-Monge, O., Velasco Bonilla, A. Z., Lafuente-Cacho, M., Peña-Carro, P. and Hernández-Jiménez, Á., Heuristic method for electric vehicle charging in a Spanish microgrid: Leveraging renewable energy surplus, Journal of Power Sources, Vol. 629, pp 235945, 2025, https://doi.org/10.1016/j.jpowsour.2024.235945
9. Singh, K. and Singh, A., Behavioural modelling for personal and societal benefits of V2G/V2H integration on EV adoption, Applied Energy, Vol. 319, pp 119265, 2022, https://doi.org/10.1016/j.apenergy.2022.119265
10. Jenn, A. and Highleyman, J., Distribution grid impacts of electric vehicles: A California case study, iScience, Vol. 25 No. 1, pp 103686, 2022, https://doi.org/10.1016/j.isci.2021.103686
11. NREL - National Renewable Energy Laboratory, Vehicle and Mobility Technologies 2024 Annual Impact Report, https://docs.nrel.gov/docs/fy25osti/91530.pdf, [Accessed: Oct. 2, 2025].
12. Chi, Y., Yu, H. and Li, Y., How do supply- and demand-side dynamics and subsidies affect the prospects for electric vehicle battery swapping services? Evidence from an evolutionary analysis, Energy, Vol. 308, pp 132922, 2024, https://doi.org/10.1016/j.energy.2024.132922
13. Lin, C., How One Chinese EV Company Made Battery Swapping Work, Harvard Business Review, 2024, https://hbr.org/2024/05/how-one-chinese-ev-company-made-battery-swapping-work
14. NIO, NIO Powers Up Third-generation Battery Swap Technology in Europe, NIO Newsroom, 2023-12-11, https://www.nio.com/news, [Accessed: Feb. 28, 2025].
15. Horak, D., Hainoun, A., Neugebauer, G. and Stoeglehner, G., Battery electric vehicle energy demand in urban energy system modeling: A stochastic analysis of added flexibility for home charging and battery swapping stations, Sustainable Energy, Grids and Networks, Vol. 37, p 101260, 2024, https://doi.org/10.1016/j.segan.2023.101260
16. Ahmad, F., Saad-Alam, M., Saad-Alsaidan, I. and Shariff, M., Battery swapping station for electric vehicles: opportunities and challenges, IET Smart Grid, Vol. 3, No. 3, pp 280-286, 2020, https://doi.org/10.1049/iet-stg.2019.0059
17. EASE - European Association for Storage of Energy, Energy Storage Applications Summary, June 2020, https://energystorageeurope.eu/publication/energy-storage-applications-summary/, [Accessed: Sept. 22, 2025]
18. Revankar, S. R. and Kalkhambkar, V. N., Grid integration of battery swapping station: A review, Journal of Energy Storage, Vol. 41, pp 102937, 2021, https://doi.org/10.1016/j.est.2021.102937

19. Zhang, X. and Rao, R., A Benefit Analysis of Electric Vehicle Battery Swapping and Leasing Modes in China, Emerging Markets Finance and Trade, Vol. 52, No. 6, pp 1414-1426, 2016, https://doi.org/10.1080/1540496X.2016.1152798
20. Diao, X. and Qiu, M., Service network design for electric vehicles with combined battery swapping and recharging, Transportation Research Part E: Logistics and Transportation Review, Vol. 208, p 104668, 2026, https://doi.org/10.1016/j.tre.2026.104668
21. Farzin, H., Zahmati, M. R. and Joorabian, M., Photovoltaic hosting capacity evaluation of distribution grid integrated with two modes of battery swap stations, Sustainable Energy, Grids and Networks, Vol. 44, pp 101951, 2025, https://doi.org/10.1016/j.segan.2025.101951
22. Cui, D., Wang, Z., Liu, P., Wang, S., Dorrell, D. G., Li, X. and Zhan, W., Operation optimization approaches of electric vehicle battery swapping and charging station: A literature review, Energy, Vol. 263, Part E, pp 126095, 2023, https://doi.org/10.1016/j.energy.2022.126095
23. Sajjadi, S. S., Moghadassi, A., Rashidizadeh-Kermani, H., Kia, R. and Shafie-Khah, M., AI-driven forecasting for battery energy management in digital twin-integrated microgrids using machine learning techniques, Journal of Energy Storage, Vol. 143, p 119556, 2026, https://doi.org/10.1016/j.est.2025.119556
24. Syafii, S., Krismadinata, K., Fahmi, F., Azizah, F. and Izrillah, I. N., Enhancing Electric Vehicle Charging Stations through Internet of Things Technology for Optimizing Photovoltaic and Battery Storage Integration, Journal of Sustainable Development of Energy, Water and Environment Systems, Vol. 13, No. 4, pp 1130609, 2025, https://doi.org/10.13044/j.sdewes.d13.0609
25. Eleksiani, A., Jackson, M., Mackey, B. and Beal, C., Renewable Energy Systems in Supporting Climate Resilience of Off-grid Communities: A Review of the Literature and Practice, Journal of Sustainable Development of Energy, Water and Environment Systems, Vol. 13, No. 3, pp 1130569, 2025, https://doi.org/10.13044/j.sdewes.d13.0569
26. Tangi, M. and Amaranto, A., Advancements in Multi-Objective Optimization for Planning and Management of Multi-Energy Systems, Journal of Sustainable Development of Energy, Water and Environment Systems, Vol. 13, No. 2, pp 1130584, 2025, https://doi.org/10.13044/j.sdewes.d13.0584
27. Lagouir, M., Badri, A. and Sayouti, Y., Multi-Objective Optimal Dispatching and Operation Control of a Grid Connected Microgrid Considering Power Loss of Conversion Devices, Journal of Sustainable Development of Energy, Water and Environment Systems, Vol. 10, No. 3, p 1090404, 2022, https://doi.org/10.13044/j.sdewes.d9.0404
28. PuLP, Optimization with PuLP, https://coin-or.github.io/pulp/, [Accessed: Sept. 22, 2025].
29. Yang, J., Liu, W., Ma, K., Yue, Z., Zhu, A. and Guo, S., An optimal battery allocation model for battery swapping station of electric vehicles, Energy, Vol. 272, pp 127109, 2023, https://doi.org/10.1016/j.energy.2023.127109
30. Alrubaie, A. J., Salem, M., Yahya, K., Mohamed, M. and Kamarol, M., A Comprehensive Review of Electric Vehicle Charging Stations with Solar Photovoltaic System Considering Market, Technical Requirements, Network Implications, and Future Challenges, Sustainability, Vol. 15, No. 10, pp 8122, 2023, https://doi.org/10.3390/su15108122
31. Electric Vehicle Database, Useable battery capacity of full electric vehicles, https://ev-database.org/cheatsheet/useable-battery-capacity-electric-car, [Accessed: Sept. 22, 2025].
32. C. Brandoni and M. Renzi, Optimal sizing of hybrid solar micro-CHP systems for the household sector, Applied Thermal Engineering, Vol. 75, pp 896–907, 2015, https://doi.org/10.1016/j.applthermaleng.2014.10.023

33. JA Solar - PV Module 410 Wp, JA Solar Technology Co., Ltd., JA Solar - PV Module 410 Wp, https://www.jasolar.com/uploadfile/2021/0602/20210602103135684.pdf, [Accessed: Sept. 22, 2025].
34. ARERA - Autorità di Regolazione per Energia Reti e Ambienti (in Italian: ARERA - Regulatory Authority for Energy, Networks and the Environment), For the consumer, https://www.arera.it/, [Accessed: Sept. 22, 2025].
35. GME - Gestore Mercati Energetici (in Italian: GME - Energy Markets Manager), Electricity, https://www.mercatoelettrico.org/en-us/, [Accessed: Sept. 22, 2025].

Paper submitted: 20.10.2025
Paper revised: 16.01.2026
Paper accepted: 14.02.2026